LINEAR, LOW-MASS, LOW-COST

A systems engineering approach to the design of a wafer handler is presented, starting with an introduction to wafer handling, followed by the corresponding requirements and lastly common system architectures. Regarding wafer-handling robots, the conclusion is that the moving robot mass increases when contamination requirements become more stringent. Moreover, robotic concepts containing a linear stroke can improve stiffness and reduce mass at the cost of contamination-sealing complexity. To conclude, the design and realisation of a low-end, low-cost magnetic bearing for high-cleanliness robotic applications is discussed.

RICK BAADE

Introduction

The front-end-of-line semiconductor manufacturing process contains multiple sequential process steps; one simplified cycle is presented in Figure 1. This cycle is repeated up to 50 times for each wafer. The wafers are transported between manufacturing tools inside a standardised container, called a front-end opening pod (FOUP), which holds 25 wafers. Before each process step, a wafer-handling module is required as an interface between the automated material-handling system (AMHS) that transports the FOUPs and the actual manufacturing equipment. The main task of the wafer-handling module is to extract wafers from a FOUP and place the wafers onto a stage or a chuck, where the actual process takes place. Key functionalities of the wafer-handling module are to transport the wafers throughout the manufacturing tools and, depending on the application, perform position aligning and/or thermal conditioning steps.

Wafer-handling modules usually contain a carrier handler to accept FOUPs, one or two robots for wafer transfer, an alignment module, and wafer storage and conditioning tables. These modules can be designed and supplied by different suppliers, therefore clear requirements on performance and interfaces are important to assure that the fully assembled system, where all modules are combined, meets the system level requirements.

AUTHOR'S NOTE

Rick Baade is a Ph.D. candidate at Eindhoven University of Technology (NL), performing his research in collaboration with VDL ETG in Eindhoven.

rick.baade@vdletg.com
www.tue.nl/cst
www.vdletg.com

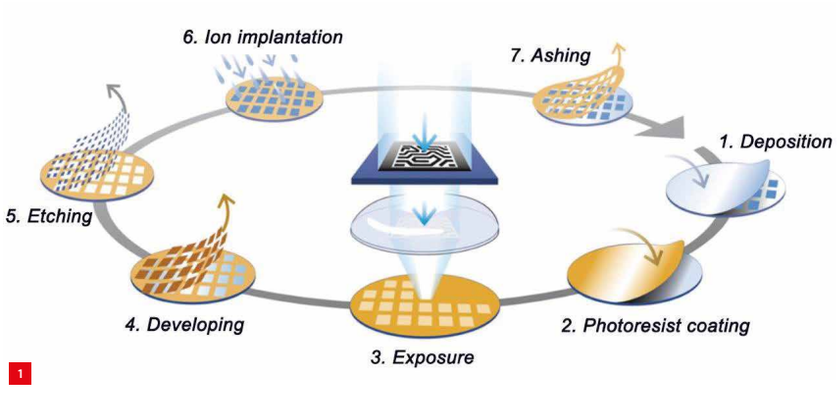

1

Front-end-of-line process cycle (ASML).

Requirements

Requirements on wafer-handling modules vary for different applications. A distinction can be made between requirements that influence the performance of the actual manufacturing process and requirements that impact productivity or yield; see Figure 2. Examples of requirements that impact the manufacturing process are position accuracy, thermal uniformity and thermal stability of the wafer. The importance of these requirements and how stringently they are specified depends on the application.

Lithography and metrology steps pose stringent requirements for wafer positioning and alignment, typically in the order of a few micrometers. For chemical and physical processes such as etching or layer deposition tools, wafer-positioning specs are less relevant and in the order of 100-500 micrometers.

Similar to the positioning accuracy specs, requirements on thermal stability and thermal uniformity are challenging for lithography and metrology tools where milli-Kelvin stability and uniformity are demanded. Wafer temperature is less relevant for other process steps; some take place at elevated temperatures of a few hundred degrees Celsius.

Requirements that impact productivity are always important, independent of the application. The complexity of semiconductor manufacturing equipment keeps increasing, following Moore's law, resulting in a continuous

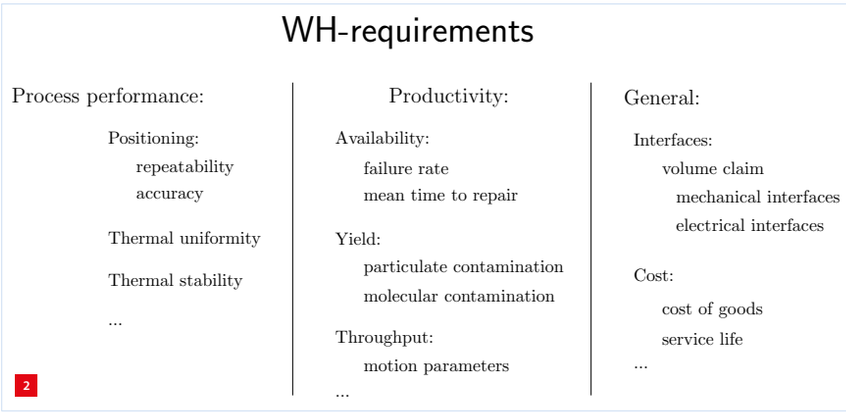

Overview of typical requirements for wafer-handling modules.

rise in equipment costs. Productivity has to increase to justify the high equipment cost. Defining productivity as a combination of throughput, availability and yield, throughput is mostly limited by the manufacturing process itself and not by the wafer-handling module, although the wafer handler is a significant productivity contributor in availability and yield. Contamination, both particulate and molecular, is believed to be a major source of yield loss. Therefore, key requirements for wafer-handling modules are defined on availability and contamination control.

Common system architectures

Three main wafer-handling architectures can be identified as corresponding to the requirements, as depicted in Figure 3. The first architecture is an equipment-front-end-module (EFEM), shown in the left of Figure 3. This type of wafer-handling module is used for most atmospheric wafer-handling applications. The EFEM acts as an interface with fabs (semicon fabrication plants) by accepting multiple FOUPs. Inside the EFEM is a wafer-handling robot provided with an extended vertical (z)-stroke to enable it to reach all FOUP positions. The robot is often placed on top of a linear axis so it can reach multiple FOUPs placed side by side. In some cases, a wafer aligner module is included for coarse alignment. Most requirements and interfaces are defined in industry standards (SEMI).

The second architecture, cluster tools, is mostly applied for in-vacuum processes and tools that apply parallel operations on multiple wafers. Examples are etching and layer-deposition tools. A cluster tool consists of a central transfer chamber that features a wafer-handling robot at the centre. The transfer chamber has a controlled environment, typically at vacuum pressure. Wafers are fed to the transfer chamber through a load lock that is often coupled to an EFEM. Multiple separate processing chambers are attached to the transfer chamber.

The final architecture is used in applications with the most stringent requirements and often provides additional functionalities, e.g. thermal conditioning. Here, the wafer-conditioning unit is integrated into the manufacturing tool. Integrated conditioning units are seen mostly in manufacturing equipment associated with the lithography step. Multiple tools that are often supplied by multiple OEMs are physically connected. For example, a wafer track that applies photoresist is coupled to the lithography tool. After the lithography step, the wafers return to the track for development. A metrology and inspection tool can also be included in this tool chain. In such a coupled system architecture, wafers are moved between manufacturing tools directly by robots without the involvement of an AMHS and FOUP.

Wafer-handling robots

Wafer-handling robots are one of the key elements of wafer-handling modules. The robots require three degrees of freedom (DoFs) for most applications, often expressed in spherical coordinates with respect to the robot base. Two in-plane DoFs are indicated by a radial distance R and an angular rotation θ. Additionally, an out-of-plane translation is required along the z-axis. The construction of most commercially available robots is based on either a selective compliance articulated robot arm (SCARA) or dual-SCARA kinematic concept, as shown in Figure 4.

The majority of the commercially available substrate-handling robots are relatively heavy compared to their payload, which is a silicon wafer with a mass of 125 g. A typical robotic arm weighs around 4.5 kg. This is due mainly to the limited height that is available to provide out-of-plane stiffness. Moreover, there is a trend towards the moving mass increasing significantly when contamination requirements become more stringent. This is due to the addition of contamination seals that significantly increase the mass, cost and complexity of the system.

The increase in moving mass negatively affects other performance requirements. High-accuracy and high-dynamic motion benefits from a high-stiffness and low-

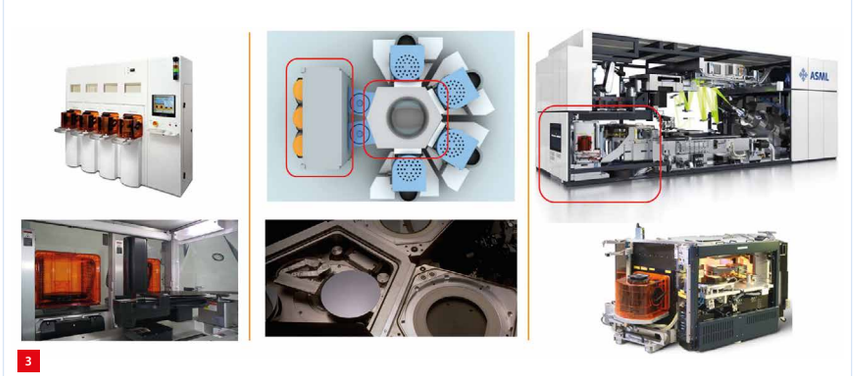

Three common wafer-handling system architectures, from left to right: Kensington Laboratories (top) and Brooks Automation (bottom); Applied Materials; ASML. See text for further explanation.

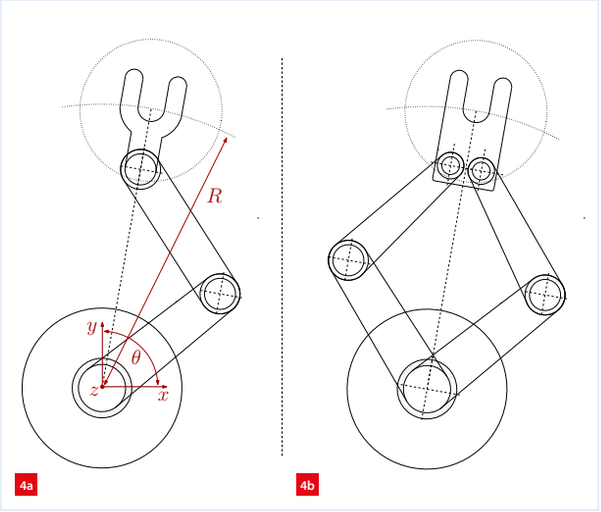

Robot architectures.
(a) SCARA.
(b) Dual-SCARA.

mass system. Minimising heat dissipation for a system with a reciprocating motion trajectory, containing a lot of acceleration and deceleration phases, favours a low moving mass. Considering the workspace and required DoFs, kinematic structures containing prismatic joints can potentially improve performance.

Magnetic bearing systems

In robotic systems, or motion systems in general, mechanical joints between moving bodies are often the main source of contamination. Typically the joints contain rolling-element bearings and contamination seals to prevent contamination from reaching the clean process environment. Examples of such contamination seals are ferrofluid, labyrinth and differentially pumped gas-purged seals. The seals contribute significantly to the mass, cost and complexity of the system. Sealing long-stroke linear joints is more difficult than sealing rotational joints, especially for in-vacuum applications. Commercially available linear contamination seals that meet semiconductor industry performance requirements have not been found.

Active magnetic linear bearings could provide an advantageous alternative to conventional rolling-element bearings [1]. As magnetic bearings are contactless, there is no mechanical friction and thus little particle generation. Moreover, there is no need for lubrication, which enables in-vacuum operation without significant outgassing. These aspects ensure that contamination seals can be omitted. The main challenges in applying magnetic bearings in high-tech in-vacuum systems lie in the minimisation of heat generation in the coils, the implementation of a stable position-feedback control loop and the linearisation of the typically nonlinear characteristics in the case of nonlinear actuators.

The remainder of this article describes the design of magnetic bearing modules intended for use in a linear guide that is part of substrate-handling robots (Figure 5).

State of the art

A significant amount of research has been done by a number of institutions on the design and control of linear motors, magnetic bearings and magnetic levitation systems for high-tech manufacturing equipment. Most of this research was driven by increasingly demanding requirements on positioning accuracy, stability and increasing velocities and accelerations (throughput). One example is the work of Trumper [2] at MIT on a high-performance linear actuator and a long-stroke magnetically levitated stage. Another is from the University of British Columbia, where Lu and Usman [3] developed 6-DoF motion stage. In 2009, Laro [4] designed an electro-magnetically suspended slider for optical disk mastering. At Philips Applied Technologies, De Klerk et al. [5] developed a stage based on e-core reluctance actuators for e-beam inspection tools.

The research described here differs from the state of the art in the sense that the focus is on a cost-effective, high-reliability solution that minimises contamination. Position accuracy requirements are less stringent and more comparable to those for conventional rolling-element bearings, in the order of 1 µm reproducibility at the end of stroke. Three main cost drivers of magnetically levitated systems have been identified, namely the motor drives, position sensors and the actual hardware such a coils and mechanics. In the proposed design, cost of these components is minimised by the development of a new sensor type and the use of linear power amplifiers.

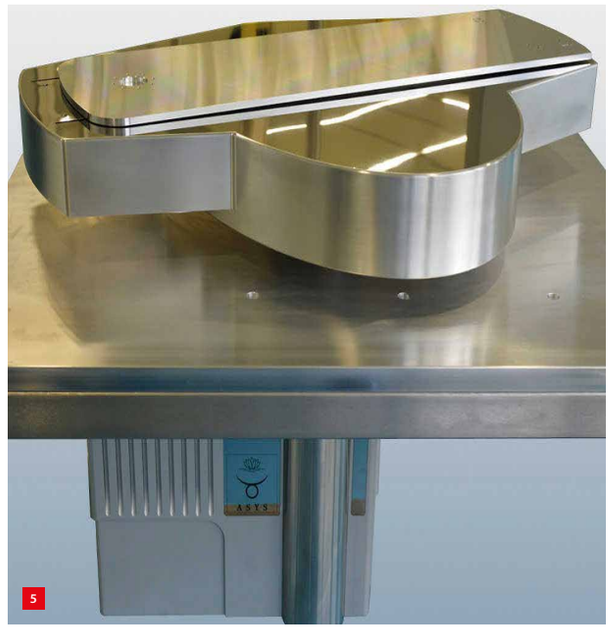

Example of a wafer-handling robot containing a linear guide (Asys Micro).

Additionally, the use of the reluctance actuation principle reduces mechanical tolerances on the coils.

Lorentz vs. reluctance

We can distinguish two types of linear electromagnetic actuators, namely the Lorentz and the reluctance types. Lorentz actuators generate a force by placing a current-carrying coil within a magnetic field. Reluctance actuators are based on the attraction force of ferromagnetic materials within a magnetic field. Table 1 shows a high-level comparison [6]. It can be concluded from this table that reluctance actuators are more efficient in terms of energy dissipation and use of volume, given the higher steepness and force density, but at the cost of increased control complexity due to the nonlinearity and negative stiffness.

Given the proposed operation of the electromagnetic actuators in a linear-bearing application with constant gap set point, the nonlinear dependence of the reluctance force on the air gap width can be linearised around the gap set point. The constant gap set point enables the short-actuation-stroke position stability requirements corresponding to conventional rolling-element bearings, in the order of 1 to 10 µm, which are believed to be feasible with reluctance-based actuators.

Proposed bearing modules

The reluctance bearing modules are based on the bearings proposed in [5] and [7]. A single magnetic bearing module is shown schematically in Figure 6 (detailed design depicted in Figure 7) and consists of a moving e-core assembly (1) and a static back iron (2). The e-core assembly consists of a laminated e-core (3), where a permanent magnet (4) is mounted on the central tooth and a coil (5) is wound around the central tooth. The static back iron is located at a distance g_1 from the e-core assembly.

This system defines a low-reluctance path where the resulting magnetic flux density in the air gap will yield a gap-dependent attraction force between the e-core and the back iron. The magnetic flux density in the air gap can either be magnified or reduced, based on the direction and magnitude of the current running through the coil, thereby controlling the magnitude of the attraction force. The actuation direction is perpendicular to the air gap (vertical direction in Figure 6). Note that this system can only generate an attraction force, thus no repelling force, between the e-core and back iron. Preloading opposite to the attraction force is required for bi-directional actuation.

Table 1
High-level comparison between Lorentz- and reluctance-type actuators.

Parameter		Lorentz	Reluctance
Linearity	[N/A]	High	Nonlinear in current and air gap
Force density	[N/m³]	Low	High
Steepness	[N²/W]	Low	High
Negative stiffness	[N/m]	Low	High
Bi-directional actuation	[-]	Yes	No
Stroke	[mm]	Long	Short

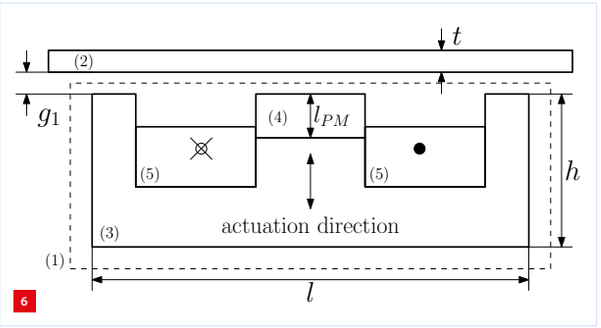

Schematic representation of a single reluctance-bearing module, comprising:
(1) bearing module;
(2) static back-iron;
(3) e-core;
(4) permanent magnet;
(5) coil.

Adjustment mechanism

Bearing modules that constrain out-of-plane DoFs can be preloaded by the weight of the payload. To minimise energy dissipation, i.e. heat generation, steady-state forces, which are required to counteract the weight of the payload, are generated by permanent magnets. Any mismatch between the static forces generated by the permanent magnets and the forces required to counteract the weight will require a

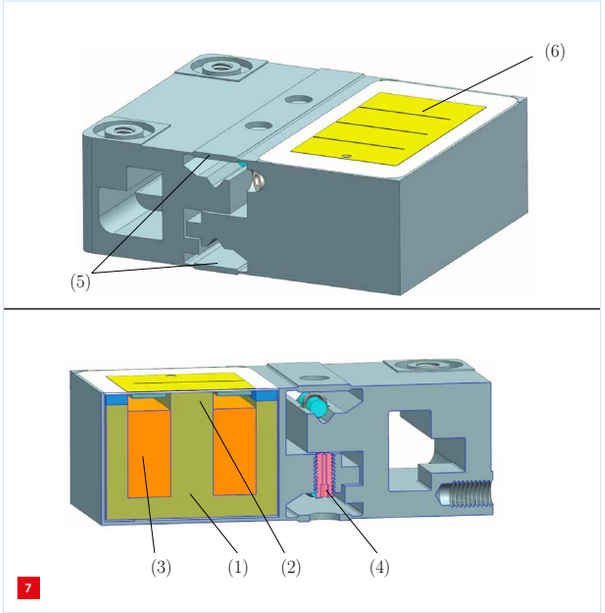

A single bearing module, highlighting the e-core (1), permanent magnet (2) and coil (3) with an adjustment mechanism consisting of two leafsprings (5) and an adjustment screw (4), and an integrated gap sensor (6).

current through the coils to correct the force balance and maintain the position set point. This will in turn lead to additional heat generation. This mismatch, for example due to tolerances on permanent-magnet parameters, can be compensated for by adjusting the air gap set point such that steady-state currents approach zero. To level the system, each bearing module has a mechanical adjustment mechanism as depicted in Figure 7, comprising two parallel leafsprings (5) with a setscrew (4). The mechanism is designed to have a stroke of 0.2 mm and an expected sensitivity of 10 µm.

Gap sensing

Given the less demanding micrometer-level positioning requirement, feedback control is based only on position or air gap sensors without additional flux sensors [8]. The sensor requires a measurement range of approximately 1 mm with an accuracy of 0.5 µm. Capacitive displacement sensors are best suited for this application. Commercially available capacitive sensors are generally cylindrical or flat shaped, with a typical minimal thickness of 4 mm. These shapes make it difficult to integrate the sensor with the magnetic bearing module and measure in the centre of the e-core (Abbe criterion).

Moreover, each sensor requires one (often tri-axial) cable for shielding, measurement signals and guard signals. In many applications, these cables need to be fed through mechanisms and rotational joints. The diameter and bending stiffness of the cables can influence the design of these rotational joints and mechanisms significantly. Additionally, these commercially available sensors are a significant cost driver for the magnetic bearing system.

Given the relatively low accuracy and dynamic-range requirements, it was feasible to design dedicated capacitive sensors. The sensor probe is integrated in the cover of the magnetic bearing (yellow surface in Figure 7), enabling gap measurement directly in the air gap. The electronics architecture includes a local pre-processing PCB that only requires two coax cables to be fed through the mechanics for up to five sensor probes, thereby significantly reducing

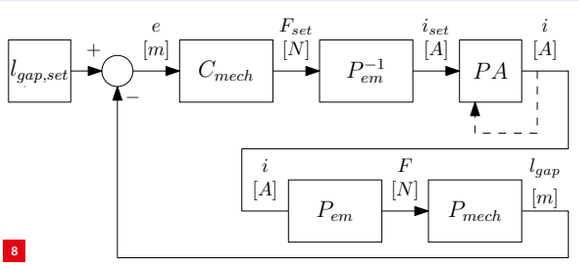

Feedback control loop showing the air gap set point, the feedback control (C_{mech}), an inverse electromagnetic model (P_{em}^{-1}), a power amplifier (PA) and the reluctance actuator itself (electromagnetic model P_{em} and mechanical model P_{mech}).

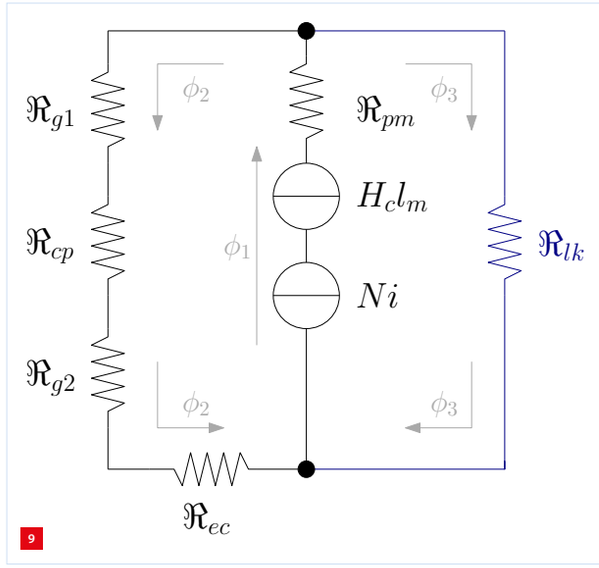

Equivalent electrical circuit containing two sources. The permanent-magnet contribution is given by the coercivity (H_c) and the magnet length (l_m), the coil contribution by the number of windings (N) and the current (i). Furthermore, several reluctance paths are shown, namely the air gap (R_g), the e-core (R_{ec}), the static counter plate (R_{cp}) and the leakage path (R_{lk})

the complexity and dimensions of the cable feedthroughs throughout the system. Ultimately, the cost of goods has been reduced by a factor 10 to 20 with respect to commercially available sensors. The accuracy was found to be within ±0.1 µm of the reference around the operating point of the magnetic bearings.

Electromagnetic system modelling

A typical feedback control scheme is shown in Figure 8. An inverse model of the electromagnetic system (P_{em}^{-1}) that maps the actuator force as a function of air gap width and current is needed to calculate the current set point. This inverse electromagnetic system is nonlinear in both current and air gap width. The actuators are used as a bearing functionality with a fixed gap set point, which allows for linearisation of the inverse model. Several analytical models

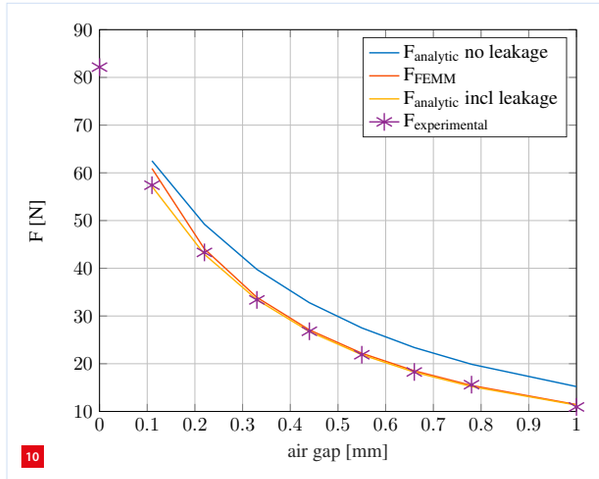

Force vs. air gap relation.

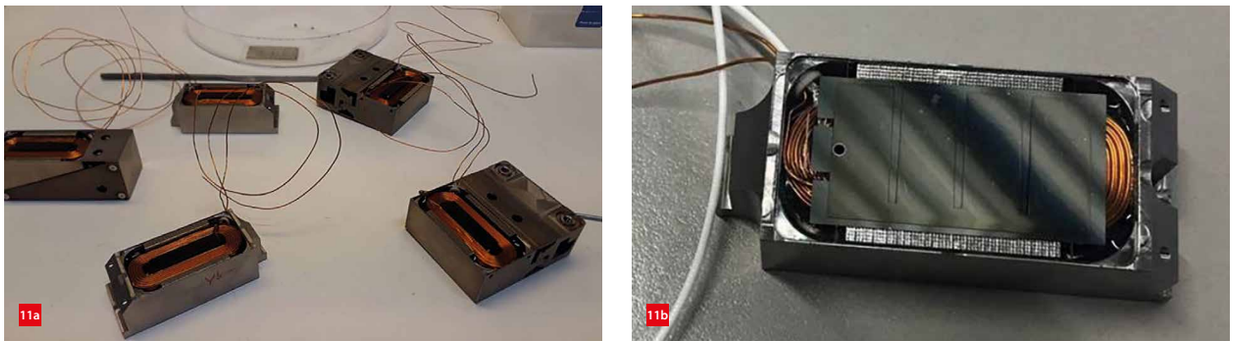

Magnetic bearing modules.
(a) Five modules during assembly.
(b) A single module with the sensor surface integrated in a glass cover. The white cable is a coaxial sensor cable and the copper wires are the coil leads.

with different levels of complexity have been evaluated and compared to finite-element modelling simulations and actual measurements.

Figure 9 shows an example of an equivalent electrical circuit [9]. The left branch describes the most basic reluctance model of a bearing module. This model comprises the coil, permanent magnet, e-core, two air gaps and the metal counterpart. The reluctance values were calculated analytically. It was found that the most basic model deviates significantly from measurements and simulations. When flux leakage is included in the model (right-hand side of Figure 9), the differences between measurements and models are within 5 per cent (Figure 10). The reluctance value of the leakage path was extracted from finite-element model simulations, at the nominal air gap value without current flowing through the coils.

Experimental validation

A number of magnetic bearing modules have been realised, as shown in Figure 11. The bearing modules consist of a titanium grade-5 housing that contains the e-core with a permanent magnet and a coil. A capacitive gap sensor is integrated in the glass cover of the bearing module. A set-up available at VDL ETG was used for experimental validation of the force vs. gap relation as described above, depicted in Figure 12. The magnetic bearing module is mounted to the aluminium frame. A steel mass is mounted to a linear bearing and translates along the actuation direction of the magnetic bearing (perpendicular to the air gap). The position of the mass, and thus the air gap width, is measured using an optical encoder (Renishaw TONiC). Additionally, a force sensor (Burster 8512) can be included to measure steady-state forces. Control and data logging are done using a Speedgoat real-time target.

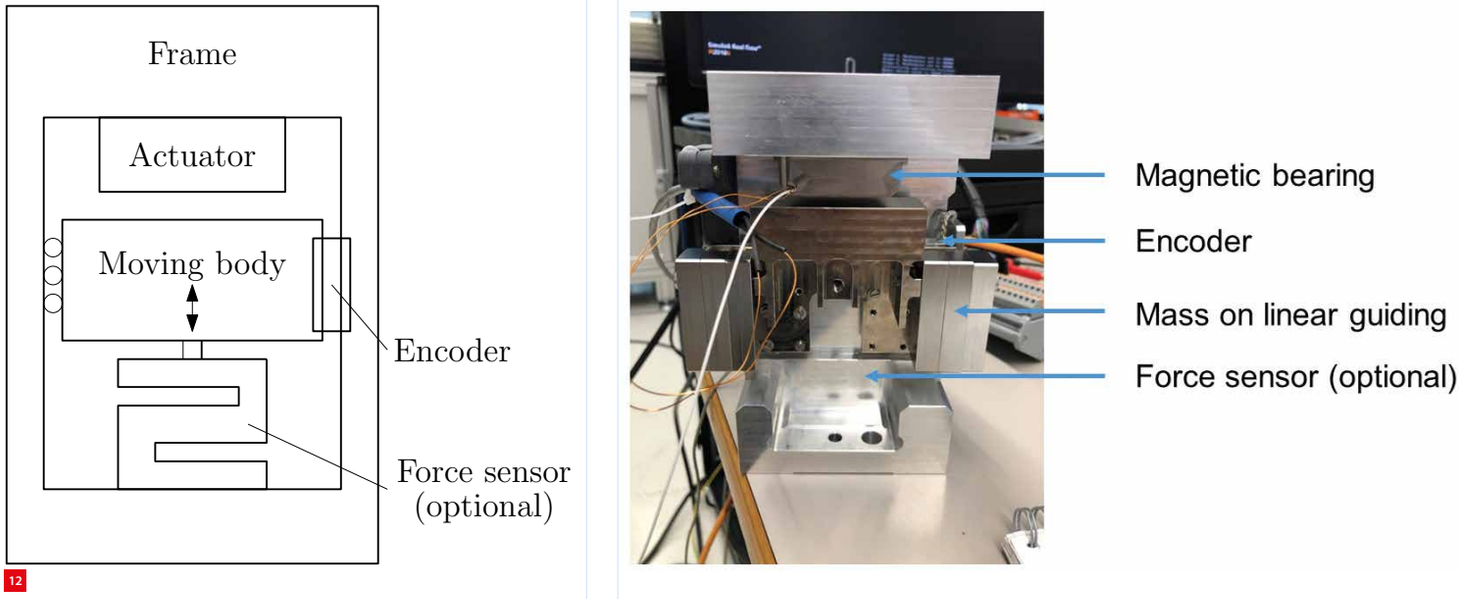

Reluctance actuator measurement set-up at VDL ETG.

Concluding remarks

The first part of this article provided an introduction to wafer-handling equipment and the corresponding requirements. The second section described the design and realisation of magnetic bearing modules, with the intended use as a linear guide as part of a novel wafer-handling robot. A demonstrator prototype of a linear guide containing seven bearing modules is currently under construction.

REFERENCES

[1] A. Peijnenburg, J. Vermeulen, and J. van Eijk, "Magnetic levitation systems compared to conventional bearing systems", *Micro-Electronic Engineering*, pp. 1372-1375, 2006.

[2] J.Y. Yoon, L. Zhou, and D.L. Trumper, "Linear stages for next generation precision motion systems", *Proceedings of the 2019 IEEE/ASME International Conference on Advanced Intelligent Mechatronics*, pp. 241-247, 2019.

[3] X. Lu, and I. Usman, "6d direct-drive technology for planar motion stages", *CIRP Annals -Manufacturing Technology*, vol. 61, pp. 359-362, 2012.

[4] D.A.H. Laro, "Mechatronic design of an electromagnetically levitated linear positioning system using novel multi-dof actuators", Ph.D. thesis, Delft University of Technology, 2009.

[5] G.Z.A. Angelo, C.P. de Klerk, and J. van Eijk, "Design of a next generation 6 dof stage for scanning application in vacuum with nanometer accuracy and mgauss magnetic stray field", *Proceedings of the 19th annual ASPE meeting*, 2004.

[6] Philips Innovation Services, "Comparative evaluation of Lorentz and reluctance actuators", technical report, 2016.

[7] R.T. Meindert, L. Norg, and J. van Eijk, "Active magnetic bearing controls strategy and calibrations", *Proceedings ASPE Spring Topical Meeting*, 2008.

[8] A. Katalenic, "Control of Reluctance Actuators for High-Precision Positioning", Ph.D. thesis, Eindhoven University of Technology, 2013.

[9] R. Hamelinck, "Adaptive deformable mirror based on electromagnetic actuators", Ph.D. thesis, Eindhoven University of Technology, 2010.